Power Handling Limit of Liquid Lithium Divertor Targets

P. Rindt[a], T.W. Morgan[b], M.A. Jaworski[c], N.J. Lopes Cardozo[a]

[a]*Eindhoven University of Technology, Science and Technology of Nuclear Fusion Group, Eindhoven, The Netherlands*
[b]*DIFFER-Dutch Institute For Fundamental Energy Research, De Zaale 20, 5612AJ Eindhoven, The Netherlands*
[c]*Princeton Plasma Physics Laboratory, Princeton NJ, USA*

Abstract

A model is formulated to make a first estimate of the maximum tolerable power of liquid lithium divertor targets, and to gain insight into their behavior in terms of lithium loss rate and surface temperature. The model, formulated as a simple analytical expression, states that the incoming power is balanced by heat conduction through the target and by the lithium which is dissipating energy in the plasma by ionizing and radiating. A target is considered to fail when the net lithium loss flux from the surface exceeds the available supply. The model is evaluated over a range of input parameters: lithium supply rate, surface layer thickness, redeposition coefficient, and dissipated energy per Li particle lost to the plasma. Based on the results, first, surface temperature locking is expected above a deposited power of ~ 10 MW/m^2. Second, lithium targets are expected to be extremely robust against power deposited during short transient events. A surface layer thickness of 50 micron is sufficient to withstand 60 MJ/m^2 vertical displacement events or 20 MJ/m^2 disruptions.

Keywords: fusion, divertor, lithium, power handling

1. Introduction

Liquid metal (LM) divertor solutions have often been proposed [1, 2, 3, 4, 5] as they potentially address issues with existing solid tungsten divertors. Important arguments for this claim are: first, the lifetime of a solid W divertor is limited by erosion [6], whereas a liquid metal target can be replenished [7]. Second, liquid lithium specifically can retain up to 100% of incoming hydrogen [8], which could lead to significantly improved plasma performance as experimentally observed with liquid lithium in NSTX and CDX-U [9, 10]. The downside is that, unless retention can be prevented, fast circulation and filtering of lithium will be unavoidable to meet tritium inventory requirements. Third, the topic of this letter, in the case of the monoblock divertor design for ITER the power handling limit is only just above the operating point. Recent work shows melting of the monoblock edges is most likely unavoidable and that the safety margin for heat load control is extremely small [11]. Better power handling is expected for LM targets due to the existence of so called "vapor shielding" [12, 7, 13]. However, the exact power handling limit has not yet been found. All of these issues are critical factors for the feasibility of commercial fusion plants.

In this work, a model is formulated to gain insight into the behavior of liquid lithium targets in terms of lithium loss rate and surface temperature, and to make a first estimate of the maximum tolerable power, beyond which components will be damaged. The model is based on theory discussed in section 2. The model itself is presented in section 3 and considers a generalized target design, which is regarded to fail when the lithium on the plasma facing surface (PFS) is depleted. Discussion and conclusion follow in section 4 and 5 respectively.

2. Theory

Lithium that is removed from the PFS dissipates energy in the plasma. This is an important contribution to the power handling capabilities of LL components. The work presented in [14], provides us with the energy dissipated per lithium particle in the plasma, ϵ_{cool}. This parameter is sensitive to the particle residence time in the plasma, τ, the electron density, n_e, and most importantly T_e.

The electron temperature can vary strongly throughout the plasma. Close to the divertor in detached scenarios T_e is in the range of 1-10 eV [15, 16], which puts ϵ_{cool} in the order of 5-10 eV. Whereas around the midplane SOL T_e is expected to be in the order of a few hundreds of eV [14], and also during transients events such as ELMs T_e can exceed 100 eV as measured and modeled for JET [17]. Correspondingly ϵ_{cool} could be as high as 500 eV.

Lastly, we must consider redeposition. A large fraction of the lost Li is expected to be ionized within the sheath region [18], and will be promptly redeposited. On top of that, lithium that is not promptly redeposited and escapes the sheath region can still be redeposited due to e.g. momentum exchange with the incoming plasma flux. In [19] it is suggested that the total redepostion fraction R in fu-

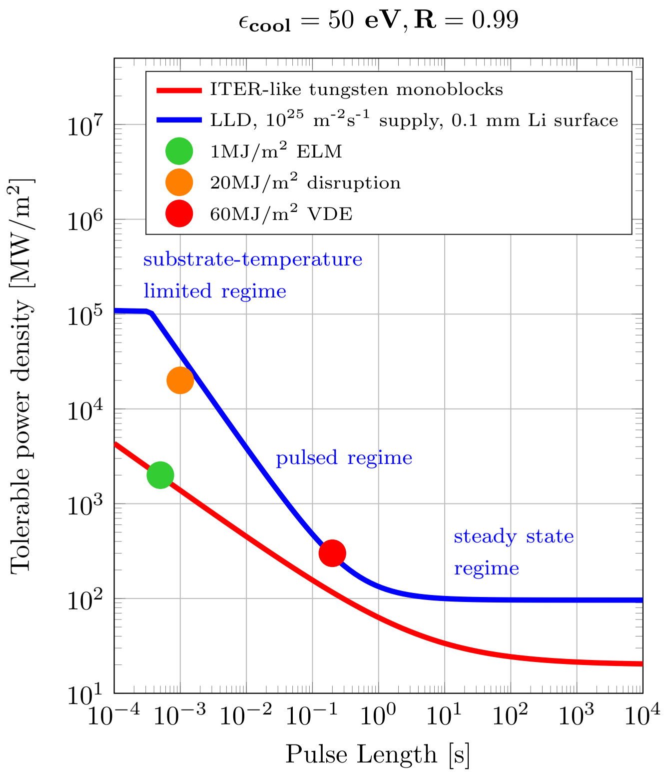

Figure 1: The maximum tolerable power density has been determined for a LL divertor target (blue) with thermal properties equal to the ITER-like monoblocks (red). This target has a lithium supply rate Γ_{supply} of 10^{25} m^{-2}s^{-1}, and a 0.1 mm top layer. ϵ_{cool} and R are taken 50 eV and 0.99 respectively. The blue curve shows three characteristic regimes: the steady state regime, the pulsed regime, and the substrate-temperature limited regime. The behavior of the former two regimes is detailed in figure 2 and 3. The -1 slope of the pulsed regime is due to the fact that the thickness of the lithium layer on the PFS corresponds to a fixed energy density which can be dissipated.

sion relevant conditions is > 0.99. Though, below $T_e < 1$ eV this could drop even to $R < 0.1$. One can imagine that in the case of prompt redeposition there is no time for the collisional radiative process that results in ϵ_{cool} to be dissipated. While not all redeposition is prompt redeposition, for practical purposes this letter will assume that all redeposited particles are indeed promptly redeposited, and that therefore ϵ_{cool} will only be dissipated by the permanently lost particles which are described by the net loss rate Γ_{net}. Effectively this is a worst case assumption.

3. Power Handling Model

A generalized divertor target is considered which consists of a tungsten substrate which is cooled on the back side. To allow comparison to the ITER monoblocks the temperature of the coolant and the effective thermal conductance of the complete target are taken $T_{cool} = 120$ C^o and $C = 13 \cdot 10^3$ Wm^{-2}K^{-1}, as derived from [20]. On the PFS sits a Li layer with surface number density N particles/m^2, which is constantly re-supplied by a uniform steady state (SS) lithium flux density Γ_{supply}. The net Li flux lost from the surface to the plasma is described as Langmuir evaporation corrected for redeposition $\Gamma_{net} = \Gamma_{vap}(1-R)$, and is constrained by the available supply, $\Gamma_{net} \leq \Gamma_{supply} + N/t$. Here t is the pulse length. The target is considered to fail when either the lithium on the PFS is depleted, or the temperature limit of the substrate material is reached.

The target is described by an energy balance in which the incoming power flux from the plasma must be balanced by 1) power dissipation via thermal conduction and 2) power dissipation by lithium entering the plasma. Contributing to the second term are ϵ_{cool}, and the evaporation energy $E_{vap} = 1.41$ eV.

$$Q_{plasma} = Q_{cond} + \Gamma_{vap}(1-R)(\epsilon_{cool} + E_{vap}) \qquad (1)$$

Here, Γ_{vap} is a strong function of T_{surf}, and Q_{cond} represents the conducted power density. The latter is composed of a term describing transient heat transfer, taken from [21], and a term for steady state heat transfer.

$$Q_{cond} = (T_{surf} - T^{\infty}_{surf})t^{-0.5}_{pulse}\sqrt{\pi C_p \rho k}/2 + C(T^{\infty}_{surf} - T_{cool}) \qquad (2)$$

Equation 1 is solved for T_{surf} as both the conducted power and lithium evaporation rate are dependent on it. C_p, ρ and k are the heat capacity, density, and thermal conductivity of the substrate respectively. Temperature T^{∞}_{surf} is the steady state surface temperature, which is obtained by solving the power balance for $t = \infty$.

A typical result is shown in figure 1. The red line is calculated considering only conductive dissipation, and represents the ITER monoblocks. The blue line indicates the behavior of a lithium target: similar to the monoblocks there is a steady state regime, where the tolerable power is set mainly by Γ_{supply}. The pulsed regime has a slope of -1 also because it is set by the available lithium, but this time the amount of lithium available on the surface during a pulse, N/t, is the dominant contribution. Naturally, the lithium in the surface layer corresponds to a fixed energy density that can be dissipated, thus resulting the -1 slope. For very short pulses the tolerable power density is again limited by the substrate surface temperature, which exceeds the tungsten melting temperature before it is sufficient to evaporate all available lithium.

The blue curve in fig. 1 is calculated for $\Gamma_{supply} = 10^{25}$ m^{-2}s^{-1}, which corresponds to a Li flux that could be supplied purely passively via only capillary forces (as for the design proposed in [22]). The influence of Γ_{supply}, surface layer thickness, ϵ_{cool}, t, and R is visualized in fig. 2 and 3. Additionally, fig. 2 shows the impact of doubling the thermal conductance of the system.

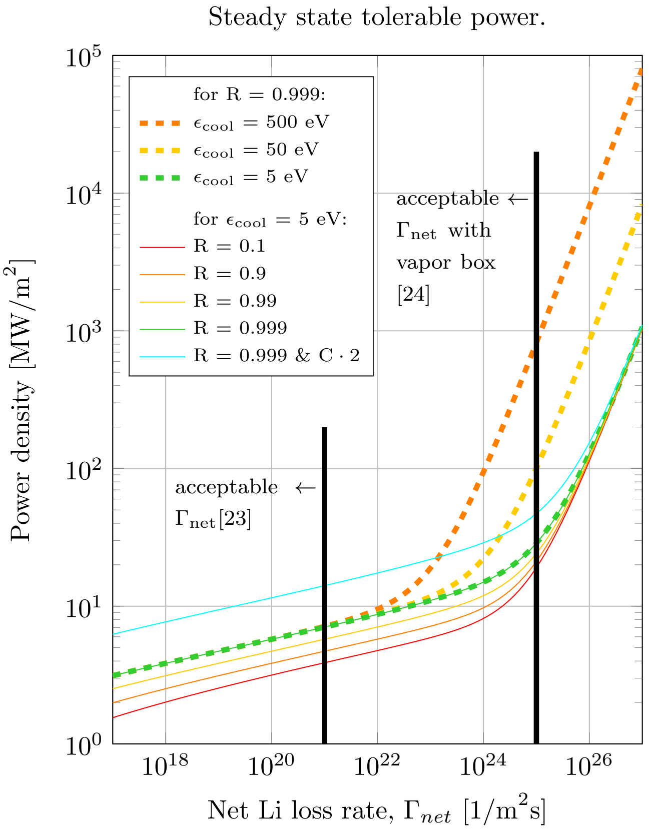

Figure 2: The steady state tolerable power density as function of Γ_{net}. A conductive regime and Li dissipation dominated regime can be observed below and above $\sim$ 20 MW m^{-2}s^{-1} respectively. Illustrated is also the influence of ϵ_{cool} (dashed), which mainly impacts the regime where dissipation via lithium is dominant, and R (solid), which impacts surface temperature to reach a given Γ_{net} and thus the conductive dissipation. The cyan line illustrates the effect of increasing the target conductance with a factor of 2. Also note that fuel dilution in the core plasma limits the allowable Γ_{net}, illustrated by the black lines.

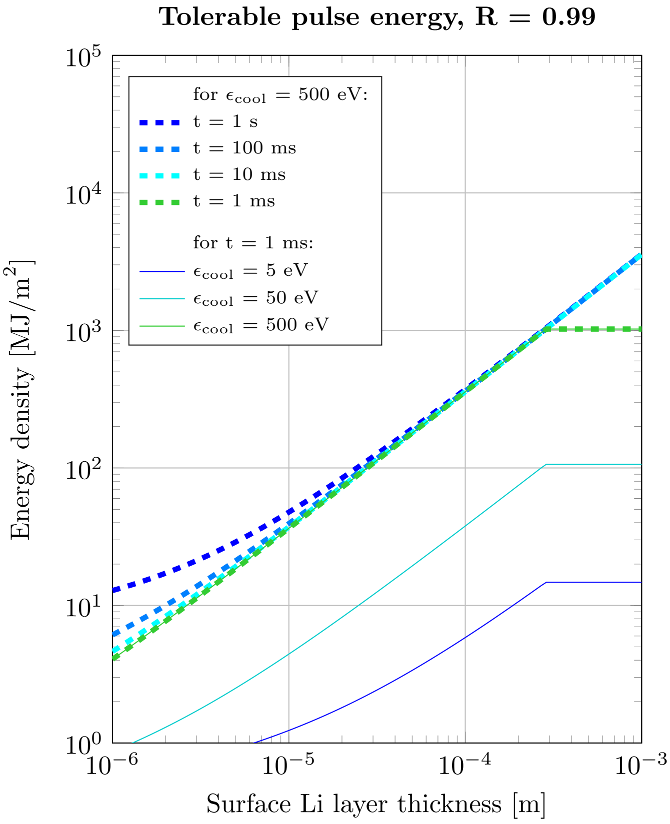

Figure 3: The energy density that can be dissipated in the pulsed regime depends linearly on the PFS LL layer thickness. For layers thinner than 10 micron conductive dissipation becomes important and dependence on pulse length t increases. For high layer thickness the substrate temperature limit is reached before all lithium can be evaporated (above 200 micron for $R = 0.99$ as presented here).

4. Discussion

In steady state (fig. 2) two "operating modes" can be distinguished clearly: a conductive and a lithium dominated mode. At respectively low load, heat is dissipated mainly via conduction. In this mode the tolerable power density can be even lower than for the monoblocks, as low surface temperature is required to maintain low net loss rates. Increasing the effective thermal conductance of the system linearly increases the tolerable load as illustrated by the cyan curve.

In the Li dominated mode orders higher power density can be absorbed, though, this mode requires net Li loss rates at least above 10^{23} m^{-2}s^{-1}. Note, that in this mode, to handle increased power density only a slight increase in surface temperature is required due to the strong dependence of evaporation on temperature. This results in a temperature locking phenomenon as indeed observed for liquid tin [25]. For lithium the locking temperature is expected to be in the range of 800 to 1000 ^{o}C.

The compatibility of these conditions with a high-performance fusion core needs to be assessed. It is estimated in [23] that Γ_{net} should not exceed $\sim 10^{21}$ m^{-2}s^{-1} to avoid fuel dilution in the core (indicated by the left black line in fig. 2). The acceptable flux density could be increased up to $\sim 10^{25}$ m^{-2}s^{-1} via strong baffling in the form of a vapor box, as calculated in [24].

In the pulsed regime dissipation by the lithium is dominant for layer thicknesses above roughly 10 micron, as indicated by the low dependence on pulse duration in fig. 3. Consequently the tolerable pulse energy density varies linearly with ϵ_{cool}, until the layer reaches critical thickness where the temperature required to evaporate all lithium during te pulse exceeds the substrate melting point. By increasing R from 0.99 in fig. 3 to 0.999, the critical thickness will be reduced from ∼200 micron to ∼30 micron.

Most notable is that disruptions, where it is expected that ϵ_{cool} lies between 50 and 500 eV, can already be withstood with layer thickness of roughly 50 micron. For VDEs this is also the case if $\epsilon_{cool} > 150$ eV. ELMs require even smaller layer thickness of ~ 0.2 micron when $\epsilon_{cool} = 500$ eV and ~ 2 micron when $\epsilon_{cool} = 50$ eV. This implies that for each ELM $\sim 10^{22}$ m^{-2} and $\sim 10^{23}$ m^{-2} lithium particles respectively are released into the plasma. Thus there may still be concerns regarding the compatibility of high Li loss rates during ELMs with the core plasma. This is not problematic for vertical displacement events (VDEs) and disruptions as the plasma is lost in these cases.

Lastly, the model considers a realistic range of $\epsilon_{cool}, R,$ and surface layer thickness, and therefore provides us with a limit to the power handing capabilities of a LL divertor target. Nevertheless, to obtain a more accurate estimate of the exact Li loss rates and power dissipation via Li, full collisional radiative modeling would be required.

5. Conclusion

Firstly, the formulated model can predict temperatures in LL divertor targets, making it a powerful engineering tool for the design of these components. Additionally, an important observation is the temperature locking effect, reducing both the peak temperature during steady state (to around 800 - 1000 ^{o}C) and during pulses. Namely, this will reduce thermal stresses, and therefore relaxes the high requirements to the strength of divertor substrate materials compared to conventional designs.

Secondly, the steady state tolerable load can be spectacularly increased compared to tungsten monoblocks, but always at the cost of high LL loss rate. To match the monoblock performance loss rates are required of $\sim 10^{25}$ $m^{-2}s^{-1}$ for $\epsilon_{cool} = 5$ eV when $R = 0.999$. Though, the loss rate for this case can be reduced ~ 3 orders of magnitude by increasing the thermal conductance of the system, and ~ 4 orders of magnitude via baffling as proposed in the vapor box concept [14]. This puts the net loss rate in the acceptable range. Nevertheless, the compatibility of specific loss rates with a high-performance fusion core should be further investigated.

Finally, regarding pulsed loads: Li layers with a thickness of 50 micron are already sufficient to withstand ELMs, disruptions, and VDEs. In the case of ELMs this may still lead to core plasma compatibility issues, but this is certainly not the case for the disruptions and VDEs as these are off-normal events, and thus the plasma is lost regardless. The ability to withstand these off-normal events is a significant and important improvement in robustness over traditional solid divertors!

6. Acknowledgement

This work has been carried out within the framework of the EUROfusion Consortium and has received funding from the Euratom research and training programme 2014-2018 under grant agreement No. 633053. The views and opinions expressed herein do not necessarily reflect those of the European Commission.

References

[1] J. W. Coenen, G. De Temmerman, G. Federici, V. Philipps, G. Sergienko, G. Strohmayer, A. Terra, B. Unterberg, T. Wegener, D. C. M. Van den Bekerom, Liquid metals as alternative solution for the power exhaust of future fusion devices: status and perspective, Physica Scripta T159 (T159) (2014) 014037. doi:10.1088/0031-8949/2014/T159/014037.
URL http://stacks.iop.org/1402-4896/2014/i=T159/a=014037?key=crossref.9c486d0b199e0e04742ae040cbb843a1

[2] D. Ruzic, W. Xu, D. Andruczyk, M. Jaworski, K. R. et Al, X. W. Jaworski M.A., Gray T.K., Antonelli M., Kim J.J., Lau C.Y., Lee M.B., Neumann M.J., R. D.N., S. J.A., M. N. Jaworski M.A., R. D.N., J. M.A., R. D. Surla V., Tung M., Xu W., Andruczyk D., Neumann M., M. D., M. R. Jaworski M.A., Gerhardt S.P., Morley N.B., Abrams T., Kaita R., Kallman J., Kugel H., R. D.N., Lithiummetal infused trenches (LiMIT) for heat removal in fusion devices, Nuclear Fusion 51 (10) (2011) 102002. doi:10.1088/0029-5515/51/10/102002.
URL http://stacks.iop.org/0029-5515/51/i=10/a=102002?key=crossref.b2156fddf3f790a36165a1cd786dec1e

[3] S. V. Mirnov, E. A. Azizov, V. A. Evtikhin, V. B. Lazarev, I. E. Lyublinski, A. V. Vertkov, D. Y. Prokhorov, Experiments with lithium limiter on T-11M tokamak and applications of the lithium capillary-pore system in future fusion reactor devices, Plasma Physics and Controlled Fusion 48 (6) (2006) 821–837. doi:10.1063/1.2405907.
URL http://www.iop.org/EJ/abstract/0741-3335/48/6/009/{%}5Cnhttp://www.iop.org/EJ/article/0741-3335/48/6/009/ppcf6{_}6{_}009.pdf

[4] L. Golubchikov, V. Evtikhin, I. Lyublinski, V. Pistunovich, I. Potapov, A. Chumanov, Development of a liquid-metal fusion reactor divertor with a capillary-pore system, Journal of Nuclear Materials 233-237 (1996) 667–672. doi:10.1016/S0022-3115(96)00010-4.
URL http://www.sciencedirect.com/science/article/pii/S0022311596000104

[5] M. a. Jaworski, a. Khodak, R. Kaita, Liquid-metal plasma-facing component research on the National Spherical Torus Experiment, Plasma Physics and Controlled Fusion 55 (12) (2013) 124040. doi:10.1088/0741-3335/55/12/124040.
URL http://stacks.iop.org/0741-3335/55/i=12/a=124040?key=crossref.5742ab9ab094e83cb3db36e4e63e010a

[6] J. Roth, E. Tsitrone, A. Loarte, T. Loarer, G. Counsell, R. Neu, V. Philipps, S. Brezinsek, M. Lehnen, P. Coad, C. Grisolia, K. Schmid, K. Krieger, A. Kallenbach, B. Lipschultz, R. Doerner, R. Causey, V. Alimov, W. Shu, O. Ogorodnikova, A. Kirschner, G. Federici, A. Kukushkin, Recent analysis of key plasma wall interactions issues for ITER, Journal of Nuclear Materials 390-391 (2009) 1–9. doi:10.1016/j.jnucmat.2009.01.037.
URL http://www.sciencedirect.com/science/article/pii/S0022311509000506

[7] S. V. Mirnov, E. A. Azizov, V. A. Evtikhin, V. B. Lazarev, I. E. Lyublinski, A. V. Vertkov, D. Y. Prokhorov, Experiments with lithium limiter on T-11M tokamak and applications of the lithium capillary-pore system in future fusion reactor devices, Plasma Physics and Controlled Fusion 48 (6) (2006) 821.
URL http://stacks.iop.org/0741-3335/48/i=6/a=009

[8] M. Baldwin, R. Doerner, S. Luckhardt, R. Conn, Deuterium retention in liquid lithium, Nuclear Fusion 42 (11) (2002) 1318–1323. doi:10.1088/0029-5515/42/11/305.
URL http://iopscience.iop.org/article/10.1088/0029-5515/42/11/305

[9] C. Taylor, K. Luitjohan, B. Heim, L. Kollar, J. Allain, C. Skinner, H. Kugel, R. Kaita, A. Roquemore, R. Maingi, Surface chemistry analysis of lithium conditioned NSTX graphite tiles correlated to plasma performance, Fusion Engineering and Design 88 (12) (2013) 3157–3164. doi:10.1016/j.fusengdes.2013.09.007.
URL http://www.scopus.com/inward/record.url?eid=2-s2.0-84888428542{&}partnerID=tZOtx3y1

[10] R. Majeski, R. Kaita, M. Boaz, P. Efthimion, T. Gray, B. Jones, D. Hoffman, H. Kugel, J. Menard, T. Munsat, a. Post-Zwicker, J. Spaleta, G. Taylor, J. Timberlake, R. Woolley, L. Zakharov, M. Finkenthal, D. Stutman, G. Antar, R. Doerner, S. Luckhardt, R. Seraydarian, R. Maingi, M. Maiorano, S. Smith, D. Rodgers, V. Soukhanovskii, Testing of liquid lithium limiters in CDX-U, Fusion Engineering and Design 72 (1-3) (2004) 121–132. doi:10.1016/j.fusengdes.2004.07.002.
URL http://linkinghub.elsevier.com/retrieve/pii/S0920379604001127

[11] J. Gunn, S. Carpentier-Chouchana, F. Escourbiac, T. Hirai, S. Panayotis, R. Pitts, Y. Corre, R. Dejarnac, M. Firdaouss, M. Kočan, M. Komm, A. Kukushkin, P. Languille, M. Missirlian, W. Zhao, G. Zhong, Surface heat loads on the ITER divertor vertical targets, Nuclear Fusion 57 (4) (2017) 046025. doi:10.1088/1741-4326/aa5e2a.
URL http://stacks.iop.org/0029-5515/57/i=4/a=046025?key=crossref.7d2d648448285fd3240c9cb62a9d3834

[12] G. van Eden, T. Morgan, D. Aussems, M. van den Berg, K. Bystrov, M. van de Sanden, Self-regulated plasma heat flux mitigation due to liquid Sn vapor shielding, Submitted To: Physical Review Letters.

[13] S. Jung, D. Andruczyk, D. N. Ruzic, Laboratory Investigation of Vapor Shielding for Lithium-Coated Molybdenum in Devex, IEEE Transactions on Plasma Science 40 (3) (2012) 730–734. doi:10.1109/TPS.2011.2181980.
URL http://ieeexplore.ieee.org/lpdocs/epic03/wrapper.htm?arnumber=6145702

[14] R. Goldston, A. Hakim, G. Hammett, M. Jaworski, J. Schwartz, Recent advances towards a lithium vapor box divertor, Nuclear Materials and Energy 12 (2017) 1118–1121. doi:10.1016/J.NME.2017.03.020.
URL http://www.sciencedirect.com/science/article/pii/S235217911630103X

[15] A. Kallenbach, M. Bernert, R. Dux, L. Casali, T. Eich, L. Giannone, A. Herrmann, R. McDermott, A. Mlynek, H. W. Müller, F. Reimold, J. Schweinzer, M. Sertoli, G. Tardini, W. Treutterer, E. Viezzer, R. Wenninger, M. Wischmeier, t. A. U. Team, P. G. et Al, T. K. et Al, K. A. et Al, Z. H. et Al, E. T. et Al, G. R, E. T. et Al, K. A. et Al, K. A. et Al, K. A. et Al, D. P. et Al, K. A. et Al, R. M. et Al, G. C. et Al, B. M. et Al, C. P. V, Piotrowicz, S. U. et Al, P. T. et Al, D. R. et Al, L. K. R, Schneider, P. D. et Al, S. P, S. P. C. W, L. A, P. C. et Al, P. T. et Al, V. E. et Al, S. J. et Al, T. G. et Al, D. R. et Al, E. W. et Al, W. M. et Al, Impurity seeding for tokamak power exhaust: from present devices via ITER to DEMO, Plasma Physics and Controlled Fusion 55 (12) (2013) 124041. doi:10.1088/0741-3335/55/12/124041.
URL http://stacks.iop.org/0741-3335/55/i=12/a=124041?key=crossref.ff6c35e3963f9fe8d849202e5d497e30

[16] M. Wischmeier, High density operation for reactor-relevant power exhaust, Journal of Nuclear Materials 463 (2015) 22–29. doi:10.1016/j.jnucmat.2014.12.078.
URL http://www.sciencedirect.com/science/article/pii/S0022311514010216

[17] D. Tskhakaya, S. Jachmich, T. Eich, W. Fundamenski, Interpretation of divertor Langmuir probe measurements during the ELMs at JET, Journal of Nuclear Materials 415 (1) (2011) S860–S864. doi:10.1016/J.JNUCMAT.2010.10.090.
URL https://www.sciencedirect.com/science/article/pii/S0022311510007580

[18] J. Allain, J. Brooks, Lithium surface-response modelling for the NSTX liquid lithium divertor, Nuclear Fusion 51 (2) (2011) 023002. doi:10.1088/0029-5515/51/2/023002.

[19] T. Abrams, Erosion and Re-Deposition of Lithium and Boron Coatings Under High-Flux Plasma Bombardment, Phd. thesis, Princeton University (2015).

[20] R. Pitts, S. Bardin, B. Bazylev, M. van den Berg, P. Bunting, S. Carpentier-Chouchana, J. Coenen, Y. Corre, R. Dejarnac, F. Escourbiac, J. Gaspar, J. Gunn, T. Hirai, S.-H. Hong, J. Horacek, D. Iglesias, M. Komm, K. Krieger, C. Lasnier, G. Matthews, T. Morgan, S. Panayotis, S. Pestchanyi, A. Podolnik, R. Nygren, D. Rudakov, G. De Temmerman, P. Vondracek, J. Watkins, Physics conclusions in support of ITER W divertor monoblock shaping, Nuclear Materials and Energy 12 (2017) 60–74. doi:10.1016/J.NME.2017.03.005.
URL https://www.sciencedirect.com/science/article/pii/S2352179116302885

[21] J. Yu, G. De Temmerman, R. Doerner, R. Pitts, M. van den Berg, The effect of transient temporal pulse shape on surface temperature and tungsten damage, Nuclear Fusion 55 (9) (2015) 093027. doi:10.1088/0029-5515/55/9/093027.
URL http://stacks.iop.org/0029-5515/55/i=9/a=093027?key=crossref.10ce3215ce783e2f5e8025718820567a

[22] P. Rindt, N. Lopes Cardozo, J. van Dommelen, R. Kaita, M. Jaworski, Conceptual design of a pre-loaded liquid lithium divertor target for NSTX-U, Fusion Engineering and Design 112. doi:10.1016/j.fusengdes.2016.08.020.

[23] T. W. Morgan, P. Rindt, G. G. van Eden, V. Kvon, M. A. Jaworksi, N. J. L. Cardozo, Liquid metals as a divertor plasma-facing material explored using the Pilot-PSI and Magnum-PSI linear devices, Plasma Physics and Controlled Fusion 60 (1) (2018) 014025. doi:10.1088/1361-6587/aa86cd.
URL http://stacks.iop.org/0741-3335/60/i=1/a=014025?key=crossref.5b0b2849de2727594a7a1941d4f95129

[24] R. J. Goldston, R. Myers, J. Schwartz, The lithium vapor box divertor, Physica Scripta T167 (T167) (2016) 014017. doi:10.1088/0031-8949/T167/1/014017.
URL http://stacks.iop.org/1402-4896/2016/i=T167/a=014017?key=crossref.afcd9baedbb2375d7775464b7e8fb91d

[25] G. G. van Eden, T. W. Morgan, D. U. B. Aussems, M. A. van den Berg, K. Bystrov, M. C. M. van de Sanden, Self-Regulated Plasma Heat Flux Mitigation Due to Liquid Sn Vapor Shielding, Physical Review Letters 116 (13) (2016) 135002. doi:10.1103/PhysRevLett.116.135002.
URL https://link.aps.org/doi/10.1103/PhysRevLett.116.135002